The 5th Joint International Conference on Multibody System Dynamics
June 24 –28, 2018, Lisbon, Portugal

Influence of Ligament Modelling on Knee Joint Kinematics with Respect to Multibody Optimisation

Evelyn Winter[1], Ingomar Schröder[1], Rainer Bader[2] and Christoph Woernle[1]

[1] *Chair of Technical Dynamics, University of Rostock, Justus-von-Liebig-Weg 6, 18055 Rostock, Germany, {evelyn.winter, ingomar.schroeder, woernle}@uni-rostock.de*

[2] *Department of Orthopaedics, University Medicine of Rostock, Doberaner Str. 142, 18057 Rostock, Germany, rainer.bader@med.uni-rostock.de*

ABSTRACT — *This study presents a subject-specific method to determine in situ both ligament stiffness and zero-load length of the collateral and the cruciate ligaments. A cadaver knee model is in-vitro tested in a robot-assisted setup to measure passive knee kinematics. A musculoskeletal multibody model with four ligaments, ACL, PCL, MCL, LCL, is built up based on the specimen test. The ligaments are modelled as nonlinear force elements, dependent from ligament parameters (stiffness and zero-load length). An optimisation algorithm is used to identify the ligament parameters which make the model reproduce the measured knee kinematics. A comprehensive parameter study is conducted for a better understanding of the influences of ligament parameters on knee kinematics. This includes a sensitivity analysis of the ligament parameters with respect to the optimisation target. The results from parameter identification show that the four ligaments are adequate to model the knee kinematics.*

1 Introduction

Knee joint kinematics depends on complex interaction between the specific geometry of the articulating surfaces and forces exerted both by adjacent soft tissues like ligaments and muscles and by applied loads. Ligament stiffness has great influence on knee stability and dynamics of the knee joint. In previous work [1] tibiofemoral ligament parameters were identified by an optimisation procedure that minimises the differences between in-vitro measured and numerically simulated tibiofemoral kinematics. For this purpose a human cadaver experiment and a sophisticated musculoskeletal multibody model were used.

Identification of ligament properties by multibody simulation of knee kinematics in combination with experimental in-vitro and in-vivo measurements is described by several researchers. Bloemker et al. [2] determined the zero-load lengths of the cruciate and collateral ligaments by comparing cadaver experiments on a mechanical knee simulator with a musculoskeletal multibody model of the experimental setup. As load case a walking cycle is considered. The zero-load lengths of the four cruciates and of the six collaterals were chosen from 15 predefined values in such a way that the root mean square differences between measurements on the knee simulator and multibody simulation are minimised. Hereby the stiffnesses of the ten ligaments were kept fixed, taken from literature [3, 4]. Guess et al. [5] built up a discrete model of the tibial articulating cartilage in a multibody environment, whereby the contact parameters were identified from measured kinematics of a cadaver specimen on a dynamic knee simulator over walking cycles. The ligament stiffnesses were taken over from Wismans et al. [4] and Blankevoort et al. [3]. The zero-load length of each ligament was determined by measuring the kinematic envelope of motion. The maximum direct distance between insertion points of a ligament over a complete flexion was calculated, and a correction percentage of 85% for the cruciate ligament bundles and 80% for the collateral ligament bundles was applied. Gasperutto et al. [6] present an optimisation

method of a multibody model against in-vivo knee kinematics measured with intracortical pins on three test persons. The knee kinematics is modelled by different kinematic models representing spatial mechanisms. The geometric parameters of the specific assemblies are obtained by an optimisation algorithm. Richard et al. [7] define a stiffness matrix to represent the compliance of the knee. The deformation energy, calculated from stiffness matrix and displacement, is minimised. Different multibody models are compared with measured knee kinematics of two healthy test persons, while ascending stairs, by using bi-planar fluoroscopy. Ottoboni et al. [8] assumed isometric behaviour for the anterior cruciate ligament (ACL), the posterior cruciate ligament (PCL) and the medial collateral ligament (MCL) and rigid articulating surfaces, and they modelled the ligaments and the constant distances of the articulating surfaces as rigid links. This leads to a parallel 5-5 mechanism of the tibiofemoral joint with one degree of freedom. In current literature the use of force-dependent musculoskeletal multibody knee models are widely used. But there are great discrepancies in the number of ligament fibres of the ligament bundles and the capsular, compare [9-13]. However these publications point out that the ACL, PCL, MCL and LCL are the most important ligament bundles that influence the knee kinematic. Some authors [14-16] use reduced number of ligament fibres.

The objective of the present study is to investigate how a measured tibiofemoral kinematics can be described by a force-dependent musculoskeletal model that comprises four ligaments (ACL, PCL, MCL, LCL according to [9-13]) and a contact model of the articulating surfaces. Such a model describes a force-dependent tibiofemoral kinematics. An optimisation algorithm is used to find the ligament parameters which make the model reproduce the measured tibiofemoral kinematics from a robot-assisted knee specimen test. The objective function describes the sum of the weighted quadratic deviations between simulation and experiment. In a systematic analysis parameters were identified that have a significant influence on tibiofemoral kinematics. The results help to understand the parameter influence from a clinical point of view and enable to define convenient weighting factors or optimisation strategies.

The paper is organized as follows. In section 2 the principle of the knee specimen test, the musculoskeletal multibody model and the optimisation procedure for knee ligament parameters that were already described in [1] are briefly summarised. In section 3 the influence of ligament stiffness and ligament zero-load length on knee kinematics is numerically analysed, and the influence on the optimisation objective function is discussed. The section ends with the results from the optimised knee kinematics against the robot-assisted knee specimen test. Three strategies for optimisation of the ligament parameters are presented.

2 Material and Methods

2.1 Robot-assisted Knee Specimen Test

The kinematics of an alcohol-fixed cadaver specimen (male, 74 years, 176 cm, 80 kg) was measured by means of a robotic test setup as shown in Figure 1. The lower right extremity was prepared with preserved ligaments and capsular structures of the knee. As described in [17] the osseous and cartilage geometry as well as the ligament attachments were reconstructed from CT and MRI scans. Anatomic landmarks were used to define tibial and femoral coordinate systems [18]. A six-axis industrial robot (TX200, Stäubli Tec-Systems GmbH, Bayreuth, Germany) is equipped with a six degree-of-freedom force-torque sensor (Omega 160, ATI Industrial Automation, Apex, North Carolina, USA). Tibia/fibula and femur were prepared and potted into mechanical fixtures using bone cement and epoxy resin, Figure 1a. The tibial component was mounted on the end-effector of the robot. The femoral side was mounted on a compliant support that is provided for force control [19]. To include the influence of the patellar ligament on knee kinematics the patella is statically loaded at the quadriceps tendon by a constant weight of 2 kg.

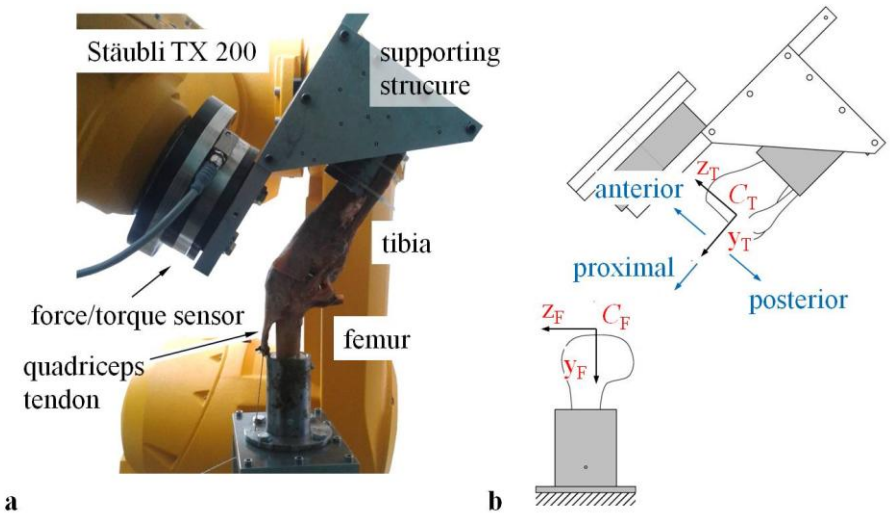

Figure 1 Setup for measurement of force-dependent knee kinematics. **a** Robot with alcohol-fixed human specimen **b** Schematic test setup with femoral bone reference system C_F and tibial bone reference system C_T.

A passive knee flexion up to 120° was analysed by moving the tibial component with respect to the femur. Hereby the flexion angle is prescribed under position control. The forces and torques along the five position coordinates were force/torque controlled with set values zero [17]. Under this control scheme the robot detects the passive knee flexion around the actual instantaneous screw axis. The position of the femur bone system C_F relative to the tibia bone system C_T, described by the displacement vector $\boldsymbol{r}_\mathrm{FT} = [\Delta x \quad \Delta y \quad \Delta z]^\mathrm{T}$ and Cardan angles $\boldsymbol{\beta}_\mathrm{FT} = [\alpha \quad \beta \quad \gamma]^\mathrm{T}$ according to Figures 1b and 2b, was measured during flexion. Thus for N prescribed flexion angles α_i a measurement vector

$$\boldsymbol{g}_i^\mathrm{test}(\alpha_i) = [\Delta x_i \quad \Delta y_i \quad \Delta z_i \quad \beta_i \quad \gamma_i]_\mathrm{test}^\mathrm{T}, \quad i = 1,\ldots,N \tag{1}$$

was recorded. In (1) describes Δx_i the medial-lateral displacement, Δy_i the distal-proximal displacement and Δz_i the anterior-posterior displacement of C_F relative to C_T, and β_i and γ_i are Cardan angles.

2.2 Multibody Model of the Knee Joint

The numerical representation of the human specimen test is realised by a multibody model according to Figure 2 and is implemented by the multibody software Simpack (V 9.7, Simpack AG, Gilching, Germany). Therein the tibiofemoral joint is modelled by a polygonal contact model which enables simulation of the roll-glide movement [8]. Pelvis, femur, tibia/fibula and patella are modelled as rigid bodies. The geometric parameters were obtained from CT scans of an alcohol-fixed human leg specimen [17]. The patellofemoral joint is modelled by a user-defined one-degree-of-freedom joint that describes the path of the patella along a femur-fixed path with the arc length s. The path is identified from a previous polygonal contact simulation of the patellofemoral joint. Wrapping of the quadriceps tendon was then implemented by a scleronomic constraint depending on the patella arc length s.

The four ligaments, MCL, LCL, ACL and PCL were modelled with non-linear dependencies of a ligament force f from the corresponding ligament strain ε according to [3]

$$f(\varepsilon) = \begin{cases} 0 & \varepsilon > 0 \\ 0.25k\dfrac{\varepsilon^2}{\varepsilon_0} & 0 \le \varepsilon \le 2\varepsilon_0, \\ k(\varepsilon - \varepsilon_0) & \varepsilon > 2\varepsilon_0 \end{cases} \tag{2}$$

with the ligament stiffness k and the strain for the transition from quadratic to linear characteristics $\varepsilon_0 = 0.015$.

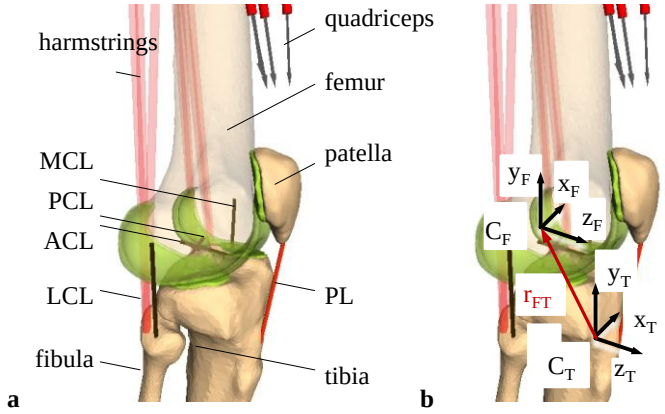

Figure 2 Musculosceletal multibody model of right knee (lateral view). **a** Anterior and posterior cruciate lig. (ACL/PCL), lateral and medial collateral lig. (LCL/MCL), patellar lig. (PL). **b** Femur bone reference system C_F and tibia bone reference system C_T .

The actual ligament strain ε is defined by the ligament length ℓ and the ligament zero-load length ℓ_0 ,

$$\varepsilon = \frac{\ell - \ell_0}{\ell_0}. \tag{3}$$

The reference strain ε^{ref} is defined as the strain of a ligament in initial knee extension at flexion 0° according to

$$\varepsilon^{\text{ref}} = \frac{\ell_{\text{ref}} - \ell_0}{\ell_0}, \tag{4}$$

whereby the reference length ℓ_{ref} is the length of the corresponding ligament at flexion 0°. A negative reference strain ε^{ref} means that, at flexion 0°, the ligament is slack, whereas a positive value indicates a pre-stressed ligament.

2.3 Ligament Parameter Identification by Multibody Optimisation

An optimisation algorithm is used to find the ligament parameters which make the musculoskeletal model from subsection 2.2 reproduce the measured tibiofemoral kinematics from the robot-assisted knee specimen test described in subsection 2.1. The model design parameters under consideration are the stiffnesses k and the reference strains ε^{ref} of the four ligaments. The reference strain ε^{ref} describes the strain of a ligament in initial knee extension at flexion 0°. Altogether these are eight model design parameters comprised in the vector $\boldsymbol{p}$. For N prescribed flexion angles α_i the multibody model calculates the five remaining displacement coordinates

$$\boldsymbol{g}_i^{\text{mod}}(\alpha_i, \boldsymbol{p}) = \left[\Delta x_i \quad \Delta y_i \quad \Delta z_i \quad \beta_i \quad \gamma_i\right]_{\text{mod}}^{\text{T}}, \; i = 1, \ldots, N, \tag{5}$$

which belong to the N equilibrium positions. The model design parameters $\boldsymbol{p}$ are determined by an optimisation algorithm in such way that the weighted squared differences between the reference position vector $\boldsymbol{g}_i^{\text{test}}(\alpha_i)$ from (1) and the simulated position vector $\boldsymbol{g}_i^{\text{mod}}(\alpha_i, \boldsymbol{p})$ from (5) are minimised. With the weighting matrix $\boldsymbol{W} = \text{diag}(w_1, \ldots, w_5)$ comprising weighting factors for the five position coordinates the objective function $Z(\boldsymbol{p})$ can be calculated by

$$Z(\boldsymbol{p}) \equiv \sum_{i=1}^{N} \Delta \boldsymbol{g}_i^{\text{T}} \boldsymbol{W} \, \Delta \boldsymbol{g}_i = \min_{\boldsymbol{p}} \tag{6}$$

with

$$\Delta \boldsymbol{g}_i^{\text{test}} = \boldsymbol{g}_i^{\text{mod}}(\alpha_i, \boldsymbol{p}) - \boldsymbol{g}_i^{\text{test}}(\alpha_i). \tag{7}$$

The optimisation problem (6) is constrained by lower and upper bounds of the M model design parameters

$$p_j^{\min} \le p_j \le p_j^{\min}, \qquad j = 1,\ldots,M. \tag{8}$$

The optimisation problem was solved using the pattern search algorithm in MATLAB R2015b. For each evaluation of the objective function (6) within the MATLAB optimisation procedure, the functions $\boldsymbol{g}_i^{\mathrm{mod}}(\alpha_i, \boldsymbol{p})$ were calculated by Simpack that was called from MATLAB.

3 Results

For an in-depth analysis of the optimisation procedure described in subsection 2.3 the influence of stiffness k and reference strain $\varepsilon^{\mathrm{ref}}$ of the individual ligaments on the tibiofemoral kinematics are analysed in subsections 3.1 and 3.2. For these numerical studies the reference values of the ligament parameters listed in Table 1 are taken over from literature.

Table 1: Stiffness parameters k from [3, 20, 21], reference strains $\varepsilon^{\mathrm{ref}}$ and reference lengths ℓ_{ref} taken from [13]

	ACL	PCL	MCL	LCL
k in N	4500	3860	8000	6000
$\varepsilon^{\mathrm{ref}}$	0.03	-0.1	0.07	0.07
ℓ_{ref} in m	0.0371	0.0296	0.0825	0.0544

In subsection 3.3 the influence of the parameters of individual ligaments on the objective function (6) is analysed. Based on the outcome from the parameter studies the identification of knee ligament parameters according to the optimisation procedure from subsection 2.1 is described in subsection 3.4.

3.1 Influence of Ligament Stiffness on Tibiofemoral Kinematics

In the study the stiffness of each ligament is varied in a range from $k = 300\,\mathrm{N}$ to $k = 9300\,\mathrm{N}$, while the remaining ligament parameters kept fixed according to the corresponding reference value in Table 1. In each of the Figures 3 to 6 the five position coordinates from (1) over the prescribed flexion angle α are shown for variations of the stiffness of one of the four ligaments. For comparison the position coordinates measured from the cadaver experiment are shown as black lines. The three diagrams on the left side of each figure show the medial-lateral displacement Δx, the anterior-posterior displacement Δy and the distal-proximal displacement Δz of the femoral bone system C_{F} relative to the tibial bone system C_{T}. The two diagrams on the right side of each figure show the Cardan angles β and γ over α. The transition of line color from pink to blue indicates increasing stiffness of the ligament under variation.

The variation of the ACL stiffness in Figure 3 shows that this parameter influences tibiofemoral kinematics between 0° and about 40° flexion while the influence is negligible over 40°. The biggest influence is seen on the anterior-posterior displacement. The influence of the PCL stiffness shown in Figure 4 starts at about 60° flexion and becomes evident especially in anterior-posterior and medial-lateral direction. The Cardan angles β and γ are affected moderately. The influence of MCL and LCL stiffnesses seen in Figures 5 and 6 are dominant with respect to the medial-lateral displacement as well as to the Cardan angles β and γ.

In all figures it can be seen the distal-proximal displacement has the lowest sensitivity with respect to the ligament stiffness as this displacement is governed by the shapes of the articulating surfaces of the tibiofemoral joint. It can be further seen that the influence of on the translational displacements is significant up to values of about 4000N only while there is most no influence beyond that value. Variation of the ligament stiffnesses alone does not enable to reach congruence with the measured data from the cadaver experiment.

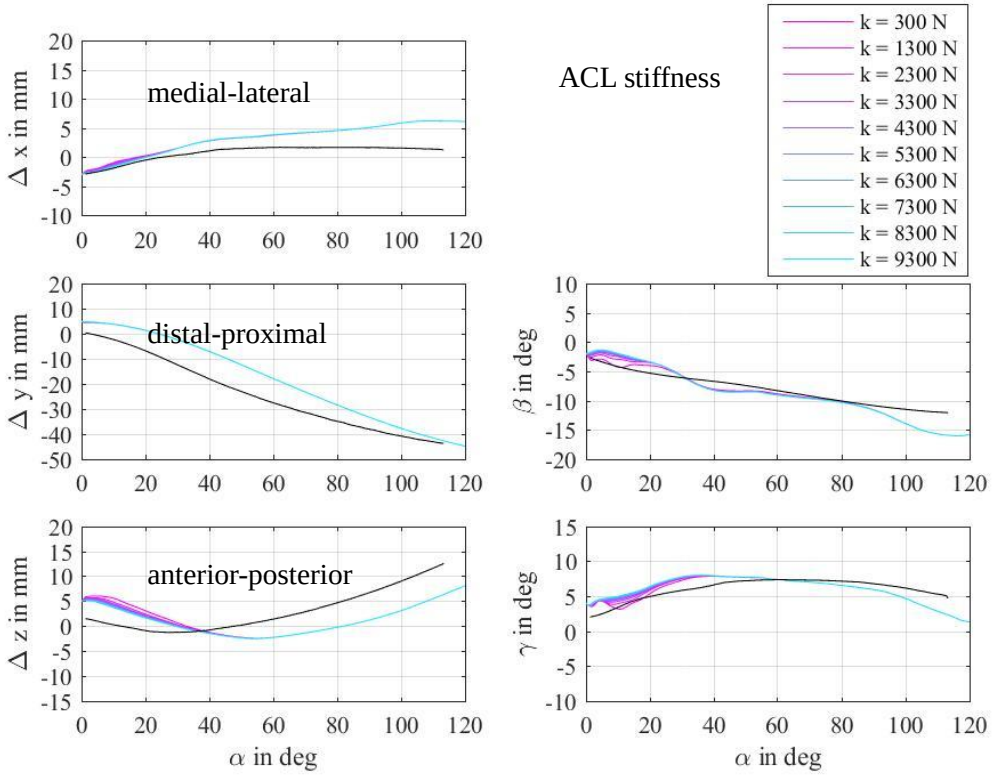

Figure 3: Influence of the ACL stiffness k_{ACL} on the position coordinates of the femoral bone system C_{F} relative to the tibial bone system C_{T} over the flexion angle α with the other ligament parameters kept constant.

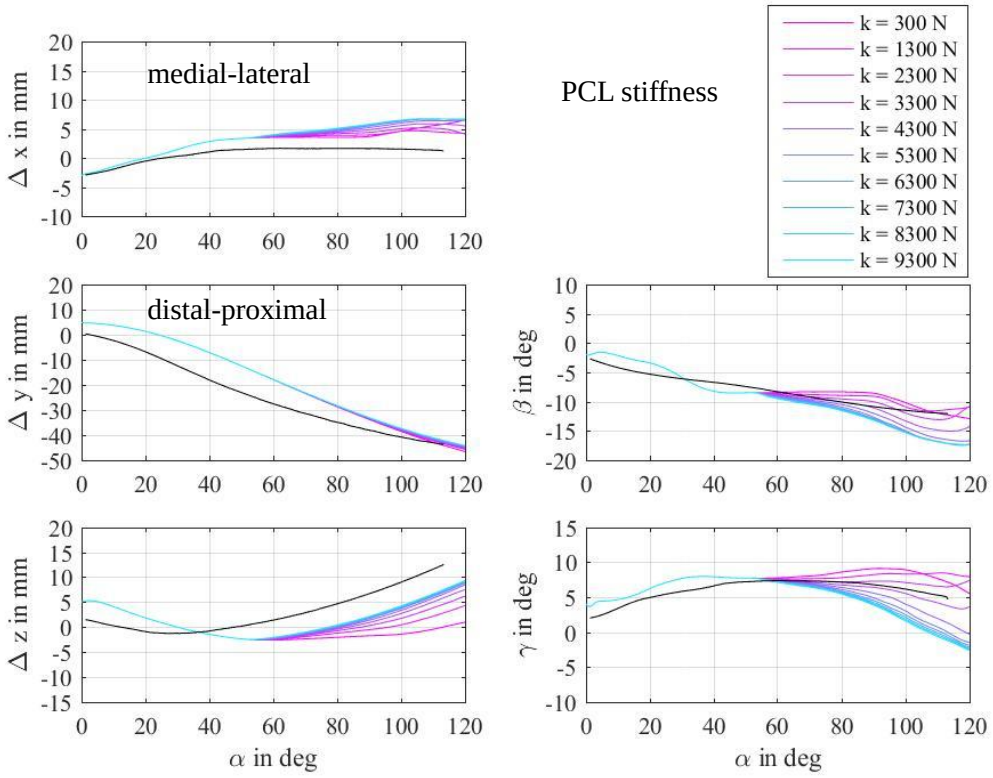

Figure 4: Influence of the PCL stiffness k_{PCL} on the position coordinates of the femoral bone system C_{F} relative to the tibial bone system C_{T} over the flexion angle α with the other ligament parameters kept constant.

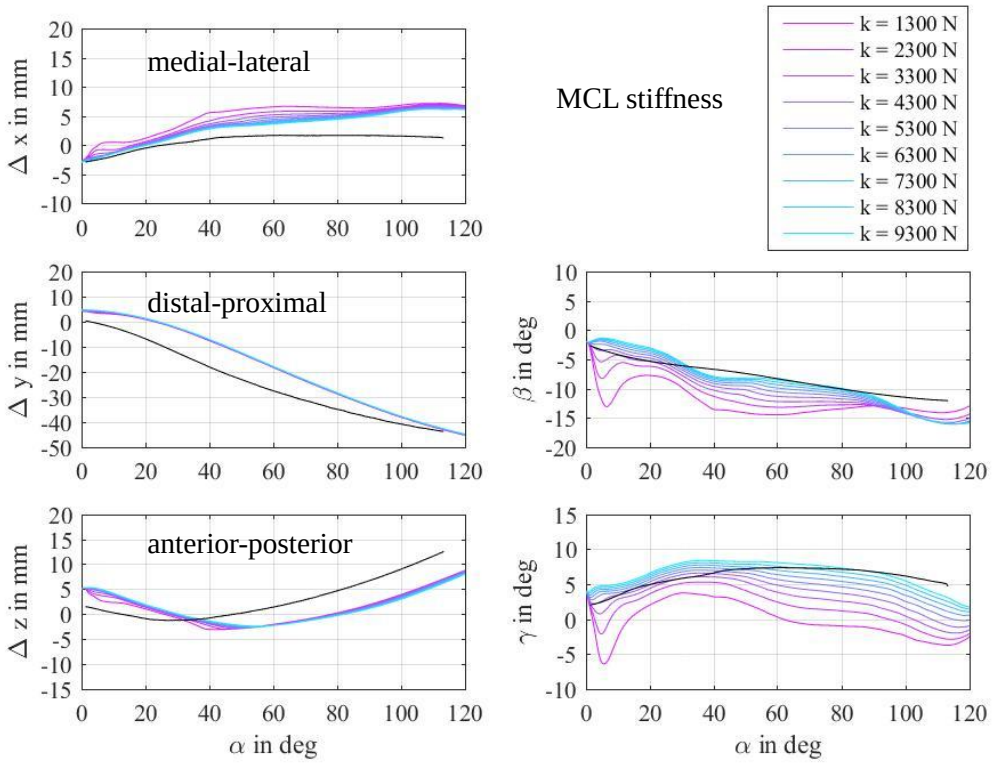

Figure 5: Influence of the MCL stiffness k_{MCL} on the position coordinates of the femoral bone system C_{F} relative to the tibial bone system C_{T} over the flexion angle α with the other ligament parameters kept constant.

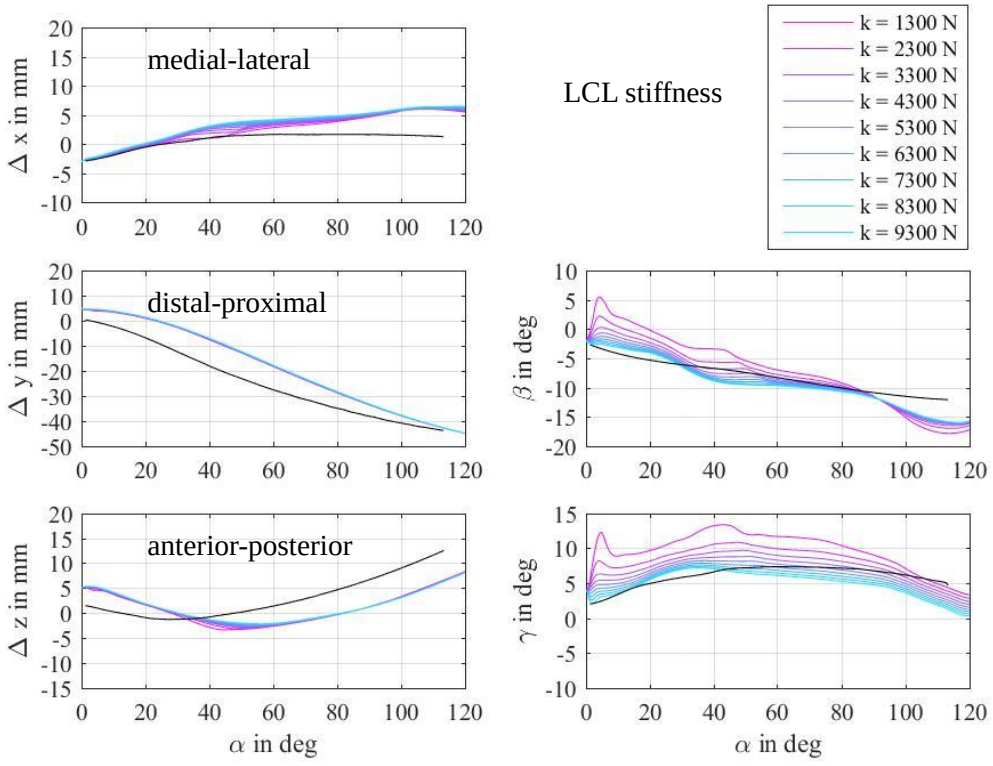

Figure 6: Influence of the LCL stiffness k_{LCL} on the position coordinates of the femoral bone system C_{F} relative to the tibial bone system C_{T} over the flexion angle α with the other ligament parameters kept constant.

3.2 Influence of Ligament Zero-Load Length on Tibiofemoral Kinematics

The influence of the zero-load length ℓ_0 on tibiofemoral kinematics is analysed in accordance with the procedures in subsection 3.1. As each ligament has an individual length ℓ_0, it is not appropriate to vary the absolute value of this parameter directly. Instead the reference strain $\varepsilon^{\mathrm{ref}}$ of each ligament is varied by increments between -0.2 to 0.2, while the reference strain of the remaining ligaments is kept constant. For given ℓ_{ref} from Table 1 and $\varepsilon^{\mathrm{ref}}$ the zero-load length is obtained from (4) according to

$$\ell_0 = \frac{\ell_{\mathrm{ref}}}{\varepsilon^{\mathrm{ref}} + 1}\,. \tag{9}$$

Figures 7 to 10 show the position coordinates of the femoral bone system C_{F} relative to the tibial bone system C_{T} over the flexion angle α. In each figure the reference strain $\varepsilon^{\mathrm{ref}}$ of ACL, PCL, MCL, and LCL, respectively, is varied while the remaining parameters are kept constant with values from Table 1. For comparison the measurements from the cadaver experiment are shown as black lines. The three diagrams on the left side of each figure show the medial-lateral displacement Δx, the anterior-posterior displacement Δy the distal-proximal displacement Δz. The two diagrams on the right side show the Cardan angles β and γ over α.

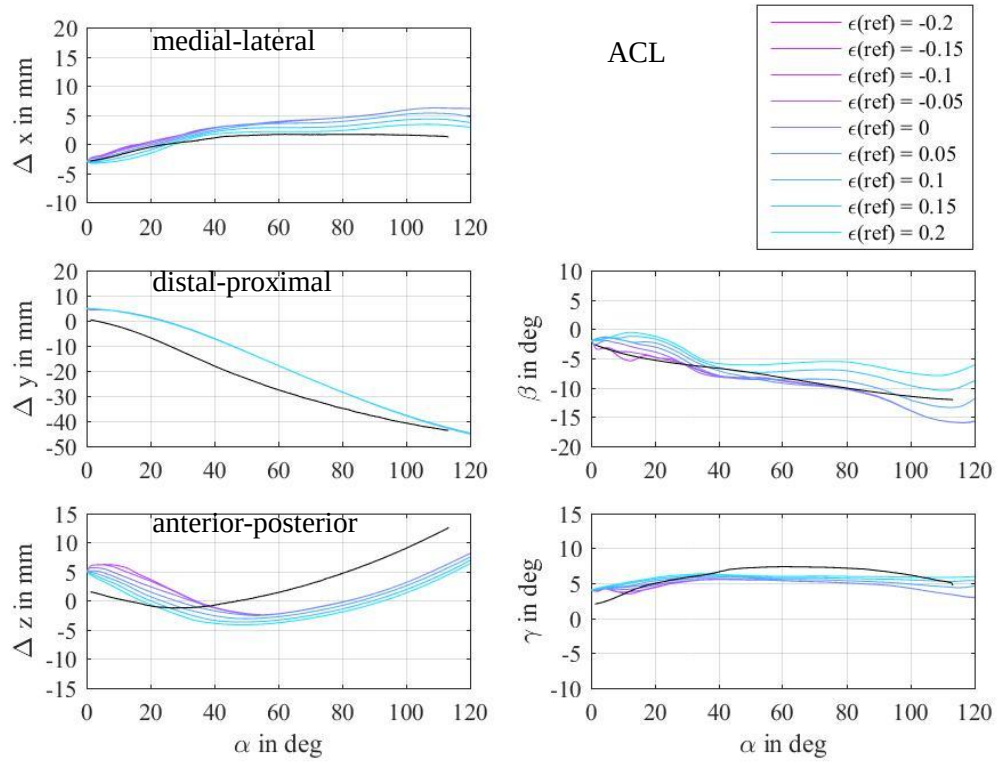

Figure 7: Influence of the ACL reference strain $\varepsilon^{\mathrm{ref}}_{\mathrm{ACL}}$ on the position coordinates of the femoral bone system C_{F} relative to the tibial bone system C_{T} over the flexion angle α with the other ligament parameters kept constant.

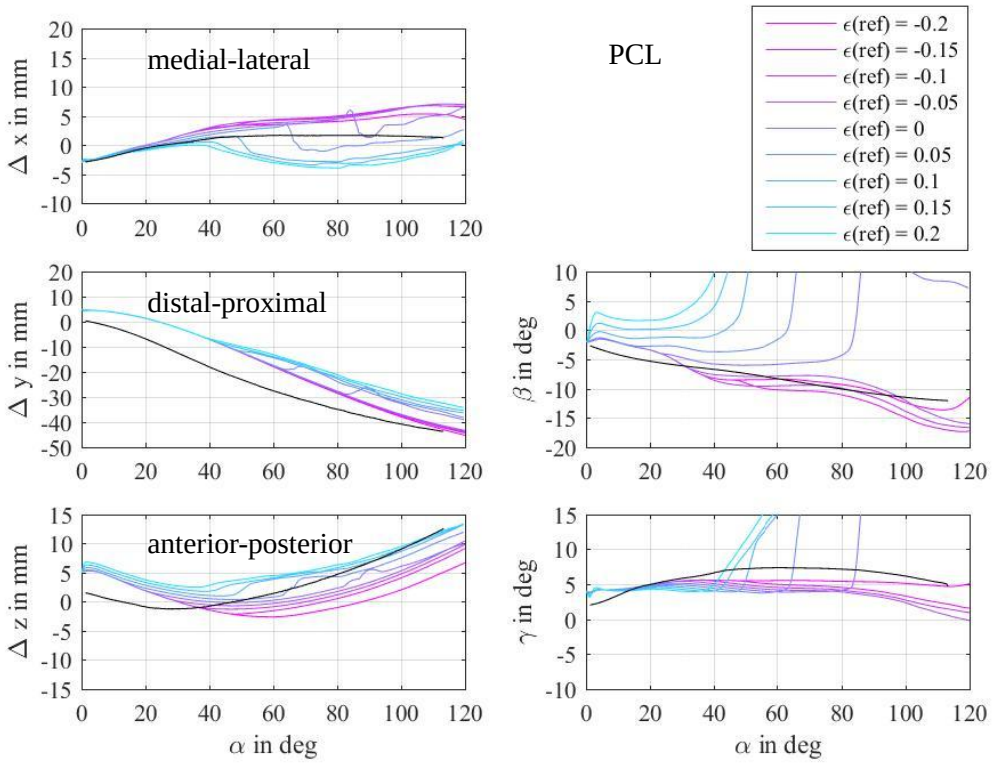

Figure 8: Influence of the PCL reference strain $\varepsilon_{\mathrm{PCL}}^{\mathrm{ref}}$ on the position coordinates of the femoral bone system C_{F} relative to the tibial bone system C_{T} over the flexion angle α with the other ligament parameters kept constant.

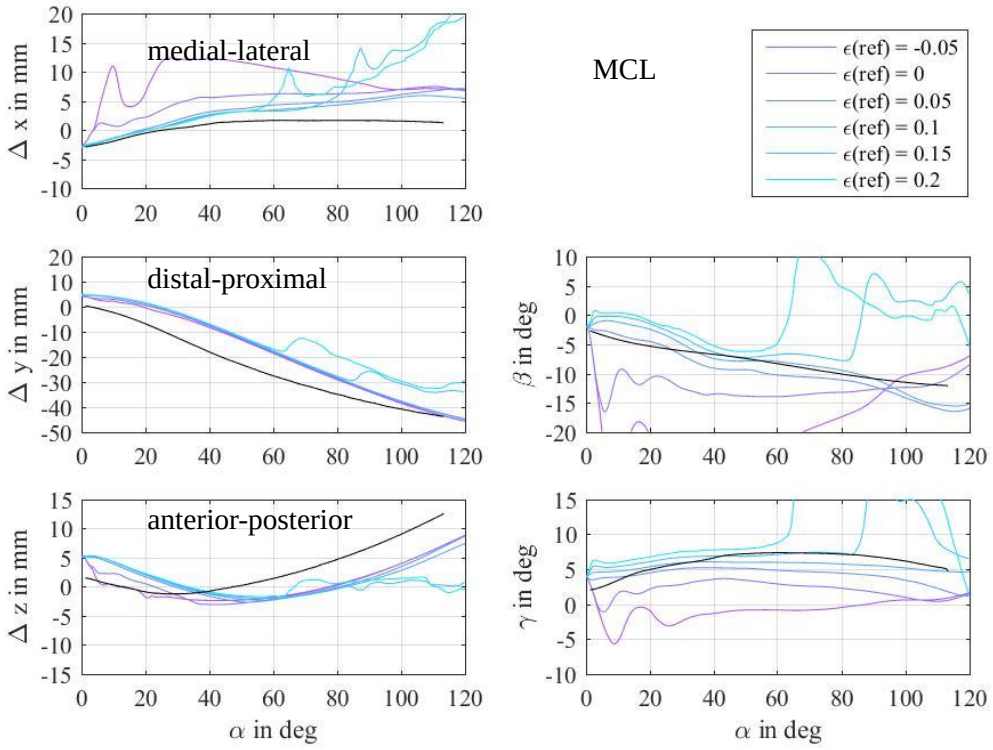

Figure 9: Influence of the MCL reference strain $\varepsilon_{\mathrm{MCL}}^{\mathrm{ref}}$ the position coordinates of the femoral bone system C_{F} relative to the tibial bone system C_{T} over the flexion angle α with the other ligament parameters kept constant.

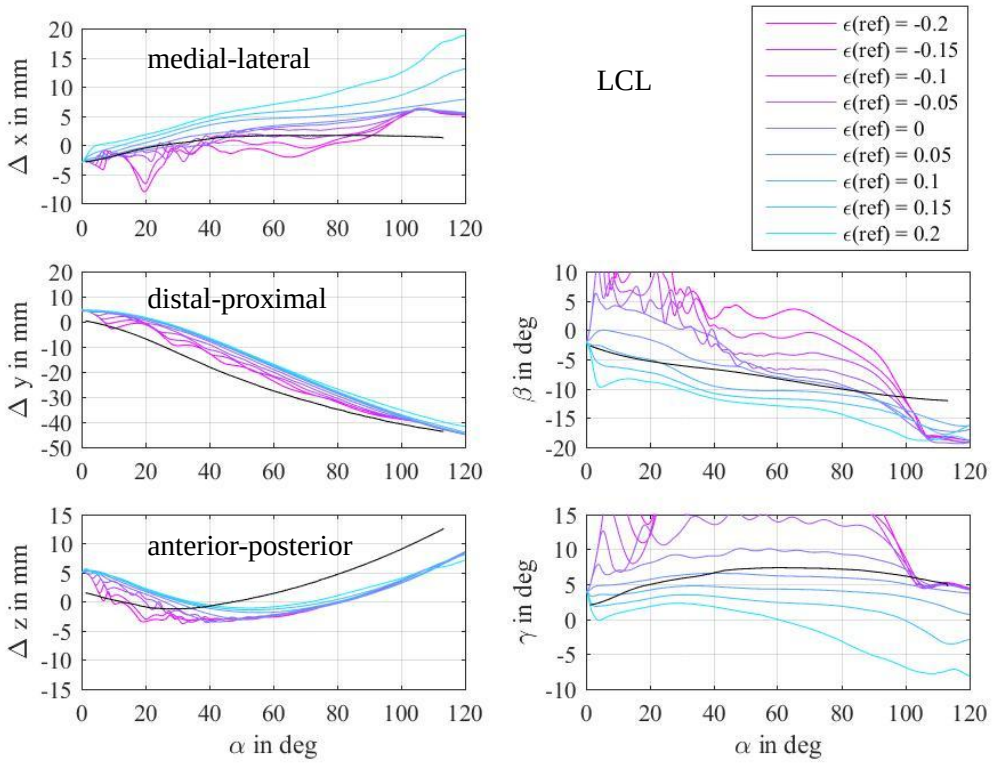

Figure 10: Influence of the LCL reference strain $\varepsilon_{\mathrm{LCL}}^{\mathrm{ref}}$ on the position coordinates of the femoral bone system C_{F} relative to the tibial bone system C_{T} over the flexion angle α with the other ligament parameters kept constant.

Altogether the tibiofemoral kinematics is more sensitive with respect to the zero-load lengths of all ligaments than with respect to the ligament stiffnesses. In particular the influence of the ACL zero-load length seen in Figure 7 is seen over the whole flexion range with the exception of the distal-proximal displacement. The variation of the PCL zero-load length in Figure 8 shows a significant influence above 40° of flexion angle. For reference strains $\varepsilon_{\mathrm{PCL}}^{\mathrm{ref}} > -0.05$ the Cardan angles β and γ indicate that the tibiofemoral kinematics becomes instable. This means that it becomes completely unphysiological. There is a small range of PCL reference strain between -0.2 and -0.05 only to obtain a physiologically reasonable knee kinematics. The zero-load length of the MCL shows, according to Figure 9, an even higher influence. Unphysiological tibiofemoral kinematics is obtained for MCL reference strains $\varepsilon_{\mathrm{MCL}}^{\mathrm{ref}} > 0.1$ and $\varepsilon_{\mathrm{MCL}}^{\mathrm{ref}} < 0.0$ For the LCL this holds for $\varepsilon_{\mathrm{LCL}}^{\mathrm{ref}} < -0.05$, see Figure 10. Further the results show that congruence between measured and modelled tibiofemoral kinematics cannot be achieved by variation of the zero-load length of one ligament only.

3.3 Influence of the Model Design Parameters on Partial Objective Functions

For a parameter identification by numerical optimisation of a simulation model it is appropriate to analyse the sensitivity of the individual parameters, here the ligament parameters, as well as their mutual independence. For example, a certain parameter that has no influence on the objective function can be omitted in the optimisation procedure in order to improve the convergence behavior and to reduce simulation time. The knowledge of the parameter sensitivities also helps to define convenient weighting factors to define an overall objective function from partial objective functions. Here the overall objective function (6) is composed by partial objective functions $Z_x, Z_y, Z_z, Z_\beta, Z_\gamma$ formulated for the five displacement coordinates according to (5). For example the partial objective function for the medial-lateral displacements Δx_i reads

$$Z_x(\boldsymbol{p}) \equiv \sum_{i=1}^{N} \left(\Delta x_i^{\mathrm{mod}}(\alpha_i, \boldsymbol{p}) - \Delta x_i^{\mathrm{test}}(\alpha_i) \right), \tag{10}$$

where $\Delta x_i^{\mathrm{test}}$ are the measurements from the robotic test setup in subsection 2.1 and $\Delta x_i^{\mathrm{mod}}$ are the values calculated by the multibody model in dependence of the model design parameters $\boldsymbol{p}$. The remaining partial objective functions are calculated in the same way as in (10).

In the following the influence of pairs of ligament parameters on the partial objective functions of the five displacement coordinates is numerically analysed. As a representative example Figure 11 shows the influence of the reference strain $\varepsilon_{\mathrm{PCL}}^{\mathrm{ref}}$ and stiffness k_{PCL} of the PCL on the five partial objective functions whereby the remaining model design parameters are kept fixed. There is a minimum zone for all partial objective functions for $\varepsilon_{\mathrm{PCL}}^{\mathrm{ref}} < -0{,}05$. The zero-load lengths have a greater sensitivity on the partial objective functions. Because the minimum zone is stretched in stiffness direction, a dependence between parameters stiffness and reference strain of the PCL with respect to the objective function cannot be identified.

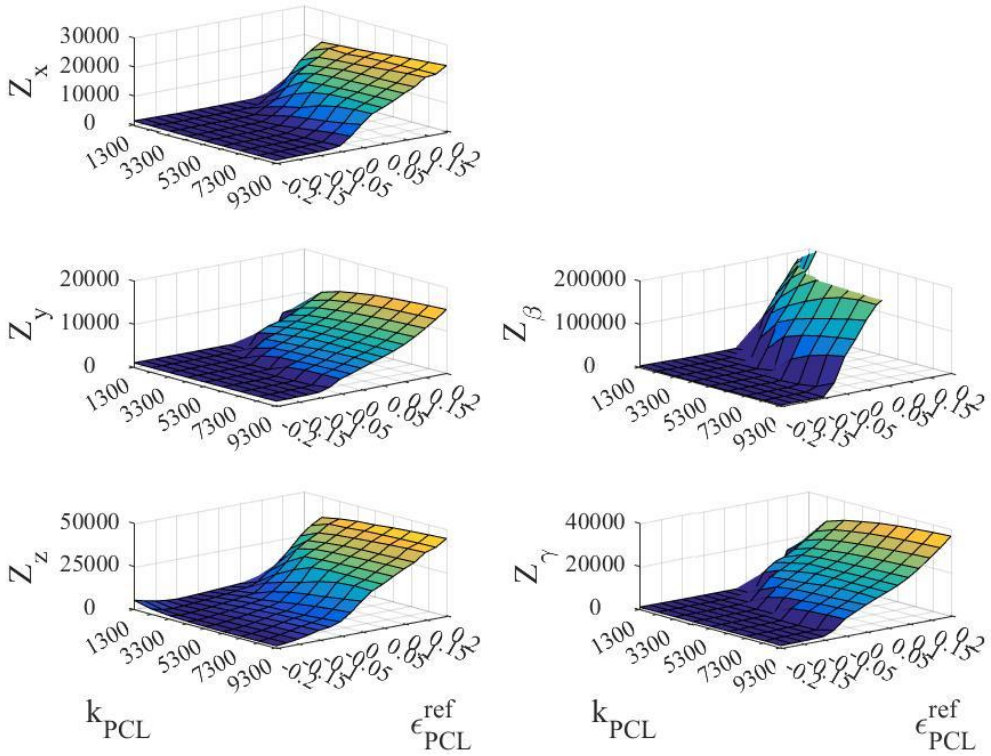

Figure 11: Influence of the PCL stiffness k_{PCL} and reference strain $\varepsilon_{\mathrm{PCL}}^{\mathrm{ref}}$ on the partial objective functions Z_i of the position coordinates of the femoral bone system C_{F} relative to the tibial bone system C_{T} with the other ligament parameters kept constant

In the same way Figure 12 shows for the LCL influence of the stiffness k_{LCL} and the reference strain $\varepsilon_{\mathrm{LCL}}^{\mathrm{ref}}$ on the five partial objective functions. The diagrams do not show a distinct minimum zone except to that belonging to angle β, which corresponds nearly to abduction/adduction.

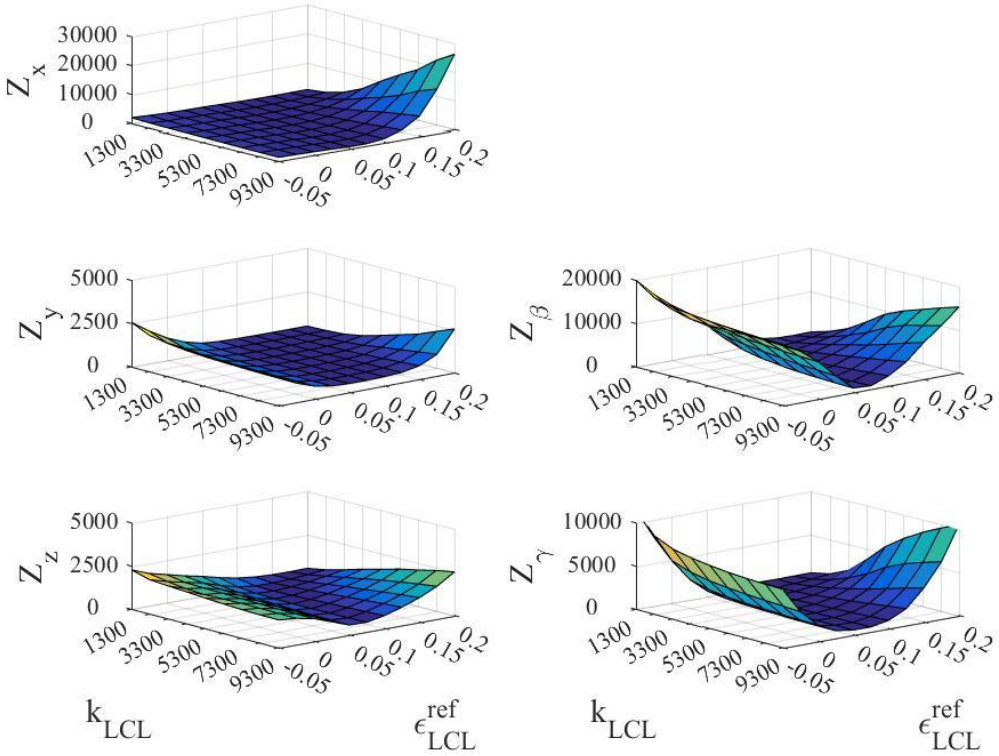

Figure 12: Influence of the LCL stiffness k_{LCL} and reference strain $\varepsilon_{\mathrm{LCL}}^{\mathrm{ref}}$ on the partial objective functions Z_i of the position coordinates of the femoral bone system C_{F} relative to the tibial bone system C_{T} with the other ligament parameters kept constant

The mutual independence of the ligament stiffnesses was also investigated. Exemplarily the correlation between the stiffness of the ACL and the PCL is analysed. In Figure 13 it can be seen that the influence of the PCL stiffness k_{PCL} on the partial objective functions is much higher than the influence of the ACL stiffness k_{ACL}. This result conforms with Figure 3 that shows a small influence of ACL stiffness on knee kinematics in the first 40° of flexion only and with Figure 4 where a significant influence of PCL stiffness beyond 60° flexion can be seen.

The effect of the variation of stiffness and reference strain on the partial objective functions is similar for all ligaments. There is a minimum valley stretched in stiffness direction. The zero-load lengths have a greater sensitivity on the partial objective functions. As the minimum valleys are mostly parallel to one design parameter axis, a dependence between parameters stiffness and reference strain of a ligament referring to the objective function cannot be identified.

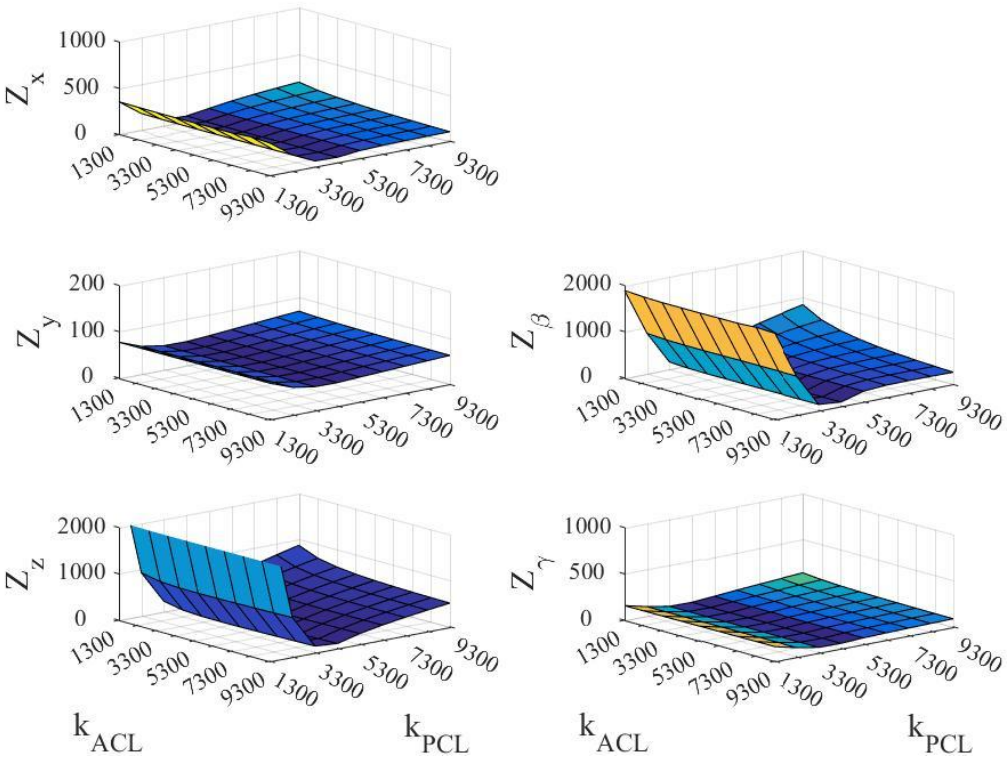

Figure 13: Influence of the ACL stiffness k_{ACL} and the PCL stiffness k_{PCL} on the partial objective functions Z_i of the position coordinates of the femoral bone system C_{F} relative to the tibial bone system C_{T} with the other ligament parameters kept constant

3.4 Identification of Knee Ligament Parameters

The multibody optimisation described in section 2.3 was performed in three ways each using different sets of model design parameters out of the altogether eight parameters, thus stiffness and zero-load length of the four ligaments, ACL, PCL, MCL, LCL. In Figure 14 the measured kinematics from the cadaver experiment is represented by black solid lines, while the results from multibody simulation with the ligament parameters from Table 1 are plotted by blue dotted lines. The three diagrams on the left side show the medial-lateral displacement Δx, the anterior-posterior displacement Δy and the distal-proximal displacement Δz of the femoral bone system C_{F} relative to the tibial bone system C_{T} over the flexion angle α in the same way as in subsections 3.1 and 3.2. The two diagrams on the right side show the Cardan angles β and γ over α.

In order to find the best parameter optimisation strategy for the given problem, the following optimisation procedures were conducted:

I. Two-step optimisation procedure:
   Step I. 1. optimising the four stiffnesses,
   Step I. 2. optimising the four zero-load lengths while taking over the stiffnesses obtained from step I.1,
II. Two-step optimisation procedure:
   Step II. 1. optimising the four zero-load lengths,
   Step II. 2. optimising the four stiffnesses while taking over the zero-load lengths obtained from step II.1,
III. Single-step optimisation procedure with all eight parameters.

For all optimisations the weighting factors for the displacements were set to 1 and for the rotations to 8 mm, whereby the dimensions of the coordinates are defined in millimeter and degree. The lower and upper bounds of the design parameters according to (8) are set for the stiffness parameters k to $k_{\min} = 300\,\mathrm{N}$ and

$k_{\max} = 10000\,\mathrm{N}$. The zero-load lengths ℓ_0 are bound by means of the reference strain $\varepsilon^{\mathrm{ref}}$ between $\varepsilon^{\mathrm{ref}}_{\min} = -0.2$ and $\varepsilon^{\mathrm{ref}}_{\max} = 0.2$.

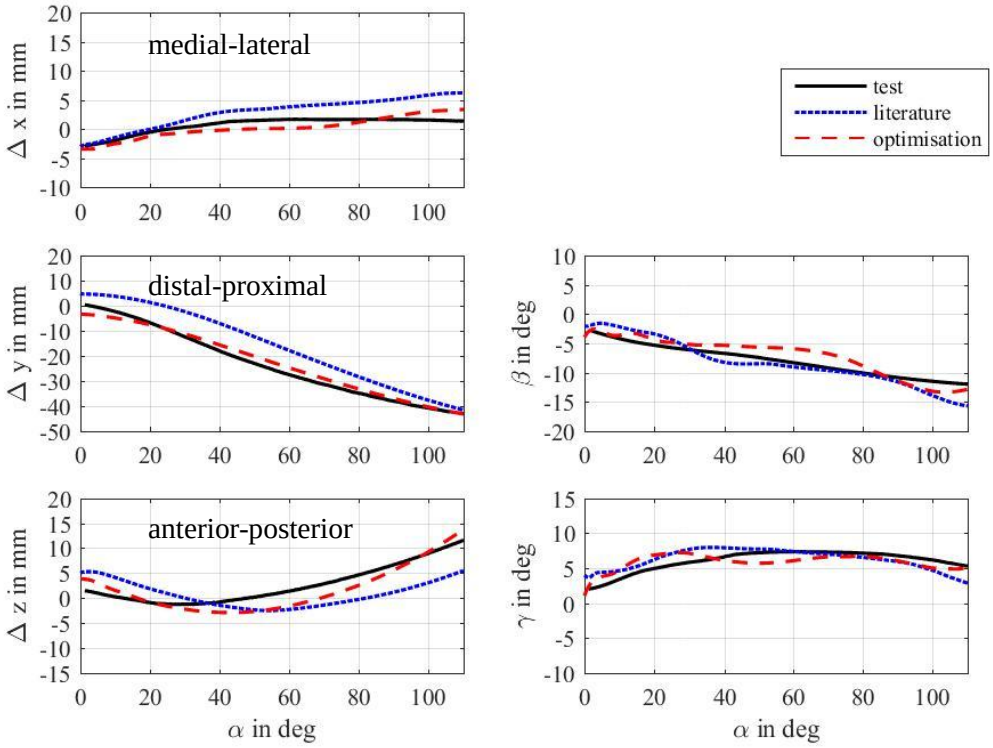

Figure 14: Position coordinates of the femoral bone system C_{F} relative to the tibial bone system C_{T} over the flexion angle α: Black solid line from cadaver measurement (test), blue dotted line from multibody simulation with reference ligament parameters from Table 1 (literature) and red dashed line from multibody simulation with ligament parameters obtained by optimisation procedure II

Optimisation procedure I takes the reference values of the stiffnesses *k* from Table 1 as initial values for step I.1, while the ligament zero-load lengths ℓ_0 are calculated from the corresponding reference strains according to Table 1. The numbers of pattern search steps and Simpack calls are given in Table 2. Optimisation procedure II is conducted in analogy to optimisation I with interchanged design parameters. According to Table 2 the numbers of pattern search steps and Simpack calls are slightly lower, while the value of the minimized objective function $Z(\boldsymbol{p})$ is slightly higher indicating a weaker optimisation outcome. Compared to the two-step optimisation procedures the single-step procedure III requires a considerably higher number pattern search steps and Simpack calls, see Table 2, in order to reach a comparable value of the objective function.

Table 2: Numbers of pattern search steps and Simpack calls for the three optimisation procedures

	pattern search steps	Simpack calls
Optimisation procedure I	**53**	**167**
Step I.1 (stiffness)	31	98
Step I.2 (zero-load length)	22	69
Optimisation procedure II	**52**	**159**
Step II.1 (zero-load length)	22	65
Step II.2 (stiffness)	30	94
Optimisation procedure III	**84**	**233**

Altogether the best approximation of the simulation model to the measured tibiofemoral kinematics could be achieved by optimisation procedure II. This is concluded by the lowest objective function. The result is shown in Figure 14 in comparison with the experiment and the simulation with the initial values from Table 1. The measured position parameters could be approximated with a considerably better accuracy. The identified ligament parameters are listed in Table 3. For the ACL, MCL and LCL the stiffnesses increase with respect to the reference values, while the stiffness of the PCL decreases. The absolute reference strains ε^{ref}, depending from the zero-load lengths ℓ_0, decrease for all ligaments. The optimisations I and III tend to result in the same values of stiffness parameters and of reference strains as in Table 3.

Table 3: Identified values of the stiffness parameters k and of the reference strains ε^{ref} obtained by optimisation procedure II

	ACL	PCL	MCL	LCL
k in N	5876	2814	8904	7048
ε^{ref}	0.037	-0.047	0.023	0.039

With this result the optimised multibody model with four ligaments provides a better approximation of the measured tibiofemoral kinematics than the 18-ligament knee model described in [1]. In addition the computational effort with 52 pattern search steps and 159 Simpack calls is much lower compared to the 95 pattern steps and 997 Simpack calls of the 18-ligament model.

4 Conclusions

The identification of knee ligament parameters based on experimental testing of cadaver specimens and multibody modeling is investigated. A force-dependent musculoskeletal knee model with four ligaments (ACL, PCL, MCL, LCL) is built up. The overall eight design parameters of the model are the stiffnesses and the zero-load lengths of the ligaments. The comparison between simulation and measurement is based on the sum of the squared differences of the tibiofemoral displacements over the flexion angle that defines the objective function for parameter optimisation. The influence of the design parameters on the partial objective functions for the displacement components is analysed. The comparison of three optimisation strategies showed that a two-step strategy with optimisation of the zero-load lengths in the first step and the subsequent optimisation of the stiffnesses requires the lowest computational effort and the best optimisation outcome. With the optimised ligament parameters the four-ligament model is able to well reproduce the measured tibiofemoral kinematics.

Acknowledgements

This research was supported by the Deutsche Forschungsgemeinschaft (DFG, German Research Foundation) – Grants BA 3347/11-1 and WO 452/10-1.

References

[1] E. Winter, R. Grawe, M. Stoltmann, P. Bergschmidt, A. Geier, R. Bader, C. Woernle, "Identification of Knee Ligament Properties by Multibody Optimisation," *Proceedings of ECCOMAS Thematic Conference on Multibody Dynamics*, June 19-22, Prague, Czech Republic, 2017.

[2] K. H. Bloemker, T. M. Guess, L. Maletsky, K. Dodd, "Computational Knee Ligament Modeling Using Experimentally Determined Zero-Load Lengths," *The Open Biomedical Engineering Journal*, vol. 6, pp. 33-41, 2012.

[3] L. Blankevoort, R. Huiskes, "Ligament-bone interaction in a three-dimensional model of the knee," *Journal of Biomechanical Engineering*, vol. 113, no. 7, pp. 263-269, 1991.

[4] J. Wismans, F. Veldpaus, J. Janssen, A. Huson, P. Struben, "A three-dimensional mathematical model of the knee-joint," Journal of Biomechanical Engineering, vol. 13, no. 8, pp. 677-685, 1980.

[5] T. M. Guess , H. Liu , S. Bhashyam, G. Thiagarajan, "A multibody knee model with discrete cartilage prediction of tibio-femoral contact mechanics," *Computer Methods in Biomechanics and Biomedical Engineering*, vol. 16, no. 3, pp. 256–270, 2013.

[6] X. Gasparutto, N. Sancisi , E. Jacquelin, V. Parenti-Castelli, R. Dumas, "Validation of a multi-body optimization with knee kinematic models including ligament constraints," Journal of Biomechanics, vol. 48, pp. 1141-1146, 2015.

[7] V. Richard, G. Lamberto, T. Lu, A. Cappozzo, R. Dumas, "Knee Kinematics Estimation Using Multi-Body Optimisation Embedding a Knee Joint Stiffness Matrix: A Feasibility Study," *PLOS one*, DOI:10.1371/journal.pone.0157010 June 17, 2016.

[8] A. Ottoboni, V. Parenti-Castelli, N. Sancisi, C. Belvedere, A. Leardini, "Articular surface approximation in equivalent spatial parallel mechanism models of the human knee joint: an experiment-based assessment," *Proceedings of I. Mech E, Part H: Engineering in Medicine*, vol. 224, no. 9, pp. 1121-1132, 2010.

[9] C. R. Smith, R. L. Lenhart, J. Kaiser, M. F. Vignos, D. G. Thelen, " Influence of Ligament Properties on Tibiofemoral Mechanics in Walking," *Journal of Knee Surgery*, vol. 29, pp. 99–106, 2016.

[10] Z. Chen, X. Zhang, M. M Ardestani, L. Wang, Y. Liu, Q. Lian, J. He, D. Li, Z. Jin, " Prediction of in vivo joint mechanics of an artificial knee implant using rigid multi-body dynamics with elastic contacts," Proc IMechE Part H: *Journal of Engineering in Medicine*, IMechE Reprints and permissions: sagepub.co.uk/journals, DOI: 10.1177/0954411914537476, 2014.

[11] D. G. Thelen, K. W. Choi, A. M. Schmitz, "Co-Simulation of Neuromuscular Dynamics and Knee Mechanics During Human Walking," *Journal of Biomechanical Engineering* , vol. 136/021033-1, 2014.

[12] M. Kia, A. P. Stylianou, T. M. Guess, "Evaluation of a musculoskeletal model with prosthetic knee through six experimental gait trials," *Medical Engineering & Physics*, vol. 36, pp. 335–344, 2014..

[13] S. Bersini, V. Sansone, C. A. Frigo, "A dynamic multibody model of the physiological knee to predict internal loads during movement in gravitational field," in *Computer Methods in Biomechanics and Biomedical Engineering*, 2015.

[14] S. Pianigiani, L. Scheys, L. Labey, W. Pascale, B. Innocenti, "Biomechanical analysis of the post-cam mechanism in a TKA: comparison between conventional and semi-constrained insert designs," International Biomechanics, vol. 2, no. 1, pp. 22–28, 2015.

[15] W. M. Mihalko, D. J. Conner, R. Benner, J. L. Williams, "How Does TKA Kinematics Vary With Transverse Plane Alignment Changes in a Contemporary Implant?," *Clinical Orthopaedics and Related Research*, vol. 470, pp. 186–192, 2012.

[16] W. M. Mihalko, J. L. Williams, " Total Knee Arthroplasty Kinematics May Be Assessed Using Computer Modeling:, A Feasibility Study," *ORTHOPEDICS*, vol. 35, no. 10, 2012.

[17] R. Grawe, M. Krentzien, M. Schulze, P. Bergschmidt, A. Geier, D. Klüß, G. Wenzel, A. Wree, R. Bader, C. Woernle, "Analysis of the elastic behavior of human knee ligaments by a robot under hybrid position-/force

control," *Proc. 4th Joint International Conference on Multibody System Dynamics (IMSD)*, June 29 - July 2, Montreal, Canada, 2016.

[18] E. S. Grood, W. J. Suntay, "A Joint Coordinate System for the Clinical Description of Three-Dimensional Motions: Application on the Knee," *Journal of Biomechanical Engineering*, vol. 105, no. 2, pp. 136-144, 1983.

[19] S. Herrmann, D. Kluess, M. Kaehler, R. Grawe, R. Rachholz, R. Souffrant, J. Zierath, R. Bader, C. Woernle, "A Novel Approach for Dynamic Testing of Total Hip Dislocation under Physiological Conditions," *PLoS One*, DOI:10.1371/journal.pone.0145798, December 30, 2015.

[20] M. G. Pandy, K. Sasaki, S. Kim, "A Three-Dimensional Musculoskeletal Model of the Human Knee Joint. Part1: Theoretical Construct.," *Computer methods in biomechanics and biomedical engineering*, vol. 1, no. 2, pp. 87-108, 1998.

[21] K. B. Shelburne, M. Pandy, "A musculoskeletal model of the knee for evaluating ligament forces during isometric contractions," *Journal of Biomechanics*, vol. 30, no. 2, pp. 163-176, 1997.